buildings

MDPI

Article

Flow Pattern and Escape Hazards of People from Flood Intrusion into the Staircase of Underground Spaces with Multiple Rest Platforms

Zhiyu Lin [1], Shengbin Hu [1,2] and Hang Lin [1,*]

[1] School of Resources and Safety Engineering, Central South University, Changsha 410083, China; 215511010@csu.edu.cn (Z.L.); hqcsut2000@163.com (S.H.)
[2] Nanning Rail Transit Co., Ltd., Nanning 530028, China
* Correspondence: hanglin@csu.edu.cn or linhangabc@126.com

Abstract: While urban underground space is being built and developed at a high speed, urban flooding is also occurring gradually and frequently. Urban water, in many disasters, has intruded into underground spaces, such as subway stations, often leading to serious casualties, in which it is crucial for people to be able to escape from the staircases. In order to enable and guide the escape of people in underground floods, a staircase model with multiple rest platforms, applicable to common entrance and exit staircase forms, was constructed. The realizable k-ε turbulence model, coupled with a volume of fluid (VOF) method, was used to simulate and analyze the flow patterns when floods of various heights intrude into the structure. The effects of rest platform settings on the ejection phenomena and flow velocity changes in flood flows were summarized. The change rule of flood flow velocity on the stairs under different flood heights and stair heights was summarized, and a linear relationship between the peak flood flow velocity and the location of the peak flow velocity point on each flight of stairs was derived. Combined with the formula of the critical conditions for people to escape upwards in the flood, the proposed escape conditions for staircases with multiple rest platforms were proposed, which provide a basis for guiding the evacuation of people in times of disaster.

Keywords: underground space; urban flooding; volume of fluid (VOF) model; hazard analysis; evacuation

check for updates

Citation: Lin, Z.; Hu, S.; Lin, H. Flow Pattern and Escape Hazards of People from Flood Intrusion into the Staircase of Underground Spaces with Multiple Rest Platforms. *Buildings* **2024**, *14*, 941. https://doi.org/10.3390/buildings14040941

Academic Editor: Eric M. Lui

Received: 20 February 2024
Revised: 23 March 2024
Accepted: 26 March 2024
Published: 29 March 2024

1. Introduction

In the past 20 years, the number of severe flooding incidents has more than doubled worldwide, making flooding the world's most frequent major disaster [1,2]. The risk of flooding in cities is rapidly increasing with climate deterioration and rapid urbanization [3–6]. Urban flooding has become a prominent problem in many countries and regions [7–10]. For example, China's urban flooding disaster in 2021 caused 59.01 million people to be affected [11]. As underground spaces, such as subway stations, are relatively closed-off, with only a few entrances and exits connected to the outside world, when flooding occurs, underground spaces can easily be flooded and trapped accidents can occur [12–15]. In recent years, flooding has intruded into subway stations in several cities in China, leading to station shutdowns and even casualties. In urban resilience theory, infrastructures such as subway stations, as carriers and important hubs, will lead to a chain of disasters in the event of a flooding accident [16,17]. On the other hand, more and more underground spaces in cities, such as subways, are being developed for mixed uses [18,19], the forms of entrances to and exits from underground spaces are diversified and undergoing complex trend developments, and the construction capacity of underground spaces is increasing; entrance and exit staircases above 8 m in height are more common (Figure 1). Because of its structural characteristics, the staircase is often the fastest flowing area in the underground space after the flood intrusion, which is the key to influence whether trapped people can escape. Therefore, studying the flow characteristics of flood intrusion into underground spaces with multiple rest platform staircases, to guide people's escape and prevent flooding accidents, can improve the comprehensive disaster prevention capability of cities, which has very realistic social benefits, as well as theoretical significance in scientific research.

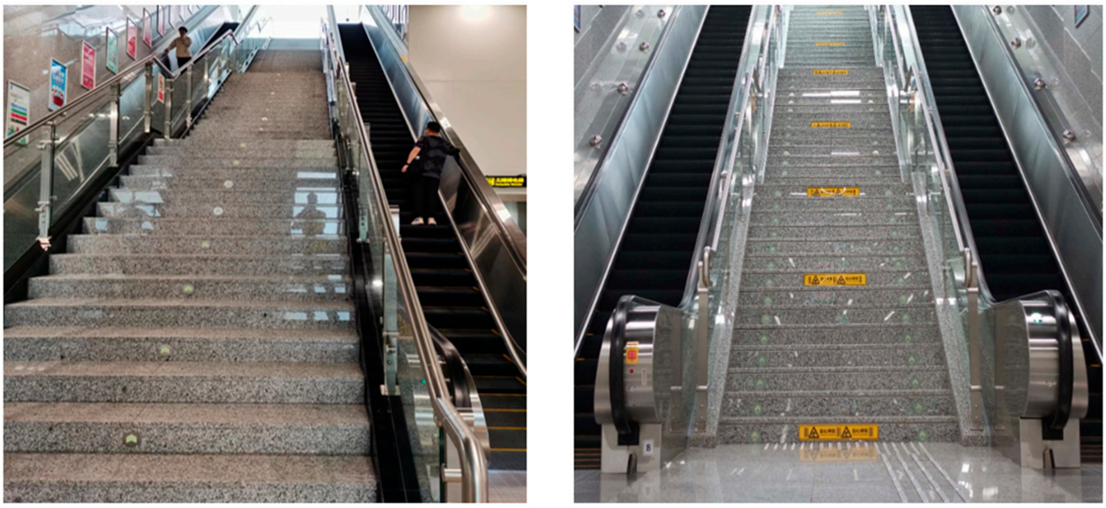

Figure 1. Common subway station entrance and exit staircase forms.

For the study of the flow pattern of flood water on the staircase and the hazard posed to people escaping, Takahashi, Nakagawa [20] proposed a falling water formula to describe the relationship between flood height and the amount of flood water flowing into the underground space. Tang, Zhou [21] simulated the evacuation process of people after the subway station flooded, analyzed the influencing factors of safe escape, and obtained the critical escape water depth for people at the station. Lin, Hu [22] built a computational fluid dynamics model of a subway station, simulated the whole process of flood intrusion, and proposed the dangerous areas and evacuation routes under different water depths and invasion passages. Inoue, Toda [23] focused on the danger zone created at the staircase when the flood intrudes into the underground space and found that the flow rate and water depth of the flood on the staircase are closely related to the escape of people; they also proposed an escape judgment function, as follows:

$$F(v,h) = v^2 h \tag{1}$$

where v and h represent the flow velocity and water depth of the flood on the staircases, respectively; when $F(v,h) > 1.5\ \mathrm{m^3/s^2}$, it is difficult for people to escape.

Ishigaki, Toda [24] modified the falling water equation by constructing a real-scale straight staircase for water flow and walking experiments and concluded that $F(v,h) = 1.2\ \mathrm{m^3/s^2}$ is the critical condition for safe escape, which resulted in a critical escape flood height of 0.3 m at the entrance of the staircases. Subsequently Ishigaki, Asai [25] considered the escape conditions of multiple types of people in underground structures on this basis and modified the escape judgment function, as follows:

$$F(v,h) = v^2 h/g + h^2/2 \tag{2}$$

Wu, Bao [26] constructed a numerical model of straight staircase flow using a smooth particle fluid dynamics approach to discretely solve the fluid problem on staircases. Shao, Jiang [27] constructed a physical test model for a staircase structure with one rest platform and analyzed the jet characteristics of the water flow after passing through the rest platform. Jiang [28] used the VOF method to establish a numerical model that can restore jet characteristics and studied the effect of multiple morphological rest platforms on the flow of water. Kim, Lee [29] verified and applied the escape judgment function (Equation (2)) to real-scale physical experiments. Hou, Chen [30] constructed a two-dimensional long staircase numerical model to study the effect of staircase slope on flood flow for both staircases and escalators. Li, Xia [31] used the large eddy simulation method to simulate water impact and to analyze the hazard of human instability at various locations on a staircase with one rest platform.

The above studies pioneered the analysis and calculation method of the flow pattern of flood water on the staircase and proposed a judgment scheme for people's escapes. However, previous research mainly focuses on straight staircases without rest platforms or staircases with one rest platform, which are models that find it difficult to meet the entrance and exit staircase height requirements of today's deeply buried underground spaces, and few studies have analyzed the influence of multiple rest platforms on the flood water flow and the possibility of escape for people on the staircase. Therefore, in this paper, for staircases with two to four rest platforms, which are more common now in the entrances and exits of underground spaces, numerical calculation was used to simulate and analyze the law of flood flows on staircases with multiple rest platforms, and to study the risks of escaping from these staircases when there are different heights of flooding in underground disasters, which provides references for flood warning and disaster prevention in underground spaces of various depths.

2. Numerical Calculation Model

2.1. Turbulence Model

Since the Navier–Stokes transport equations are relatively difficult to solve directly in the face of larger-scale turbulence problems, the Reynolds-averaged Navier–Stokes (RANS) method and large eddy simulation (LES) method are often used to compute turbulence problems in computational fluid dynamics [32–34]. The use of the RANS method has the advantage of a relatively low computational cost and more plausible results from steady-state calculations, when compared to the LES method, for solving larger scale turbulence problems. At the same time, the RANS method requires a higher degree of meshing. However, in this paper, due to the overall simplicity of the staircase structure, the mesh could be refined to achieve the desired accuracy while maintaining the quality of the mesh. On the other hand, the RANS method is widely used in the practice of hydraulic flow engineering calculations [35], and its basic continuity and momentum equations are given below, in Equations (3) and (4). The *k*-*ε* model, *k*-*ω* model, and Reynolds stress equation model (RSM), etc. are commonly used in turbulence models. The realizable *k*-*ε* turbulence model, as an improved model of the standard k-ε model, introduces a more reasonable turbulent viscosity equation and energy dissipation rate transfer model, which allows it to more accurately simulate the flow field state in the upper part of the water flow during flood intrusion into the staircase [28,36,37]. Its *k*-*ε* turbulence equations are given below, in Equations (5) and (6).

$$\frac{\partial \rho}{\partial t} + \frac{\partial(\rho u_i)}{\partial x_i} = 0 \tag{3}$$

$$\frac{\partial(\rho u_i)}{\partial t} + \frac{\partial(\rho u_i u_j)}{\partial x_j} = -\frac{\partial P}{\partial x_i} + \frac{\partial}{\partial x_j}[2S_{ij}(\mu + \mu_t)] \tag{4}$$

where ρ and t are density and time; u_i, u_j and x_i, x_j are velocity components and coordinates, respectively; P is the pressure; μ is the molecular viscosity; S_{ij} is the average strain rate, $S_{ij} = \frac{1}{2}(\frac{\partial u_i}{\partial x_j} + \frac{\partial u_j}{\partial x_i})$; μ_t is the turbulent viscosity coefficient. $\mu_t = \rho C_\mu \frac{k^2}{\varepsilon}$; and, in the realizable *k*-*ε* turbulence model, C_μ is the function of the average strain rate and curl.

$$\frac{\partial(\rho k)}{\partial t} + \frac{\partial(\rho k u_j)}{\partial x_j} = \frac{\partial}{\partial x_j}\left[\left(\mu + \frac{\mu_t}{\sigma_k}\right)\frac{\partial k}{\partial x_j}\right] + G_k + G_b - \rho\varepsilon - Y_m \tag{5}$$

$$\frac{\partial(\rho\varepsilon)}{\partial t} + \frac{\partial(\rho\varepsilon u_j)}{\partial x_j} = \frac{\partial}{\partial x_j}\left[\left(\mu + \frac{\mu_t}{\sigma_\varepsilon}\right)\frac{\partial\varepsilon}{\partial x_j}\right] + \rho C_1 S\varepsilon - \rho C_2 \frac{\varepsilon^2}{k + \sqrt{v\varepsilon}} + C_{1\varepsilon}\frac{\varepsilon}{k}C_{3\varepsilon}G_b \quad (6)$$

where k and ε are the turbulent kinetic energy and dissipation rate, respectively; σ_k and σ_ε are the turbulent Prandtl number of the turbulent kinetic energy and dissipation rate, respectively; G_k is the turbulent energy generated by the mean velocity gradient; G_b is the turbulent energy generated by buoyancy; Y_m denotes the influence term of compressible turbulent pulsation expansion; $C_1 = \max\left[0.43, \frac{\eta}{\eta+5}\right]$, $\eta = S\frac{k}{\varepsilon}$; $S \equiv \sqrt{2S_{ij}S_{ij}}$; v is the coefficient of molecular motion viscosity; and $C_{1\varepsilon}$ = 1.44, C_2 = 1.9, and $C_{3\varepsilon}$ = 1.0.

2.2. Volume of Fluid (VOF) Method

The VOF method is suitable for solving the free surface tracking description problem for two or more immiscible fluids, wherein only one fluid (e.g., air) is compressible [38–40]. The method has been validated and is widely used in wave simulations [41–45], dam-break models [38,46], and multiform step–fall simulations [47–49]. The core idea of the VOF method is to set the volume fraction as an α function, to characterize the proportion of fluid occupancy in a cell. A cell with an α value between zero and one must contain the gas–liquid intersection. The volume fraction continuity equation in the VOF method is given in Equation (7), as follows:

$$\frac{\partial\alpha}{\partial t} + u_i\frac{\partial\alpha}{\partial x_i} = 0 \quad (7)$$

In this paper, the realizable k-ε turbulence model coupled with the VOF method was used to solve the RANS equations, in which the cell is filled with flood water when α = 1, and the cell is filled with air when α = 0. Referring to previous step flow analyses [29,50], the isosurface where α = 0.1 is considered as the interface between flood and air.

The interface reconstruction algorithm in this paper was based on the PLIC (piece-wise liner interface construction) method proposed by Youngs [51], which uses a straight line $(n_x + n_y = \beta)$ in a cell to approximate the interface between the two phases instead, whereby the flow rate through each cell interface is determined, as well as the value of the volume fraction α in the cell containing the water–air interface (Figure 2).

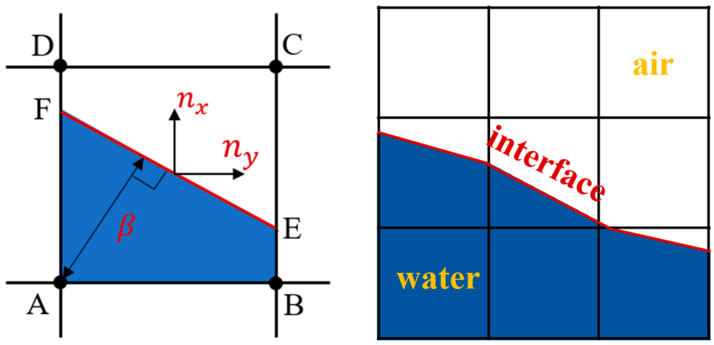

(**a**) (**b**)

Figure 2. Interface reconstruction algorithm. (**a**) Schematic of PLIC interface reconstruction method; (**b**) water–air interface generation result.

2.3. Solution Methods

In solving differential equation problems, several methods have been developed to cope with different solution objects. For example, the meshless generalized finite difference method is applied to the stress analysis of three-dimensional composites [52]; the generalized Bézier multi-step method [53] and the differential quadrature method [54] for are used to solve the initial and boundary value problems of differential equations.

The finite volume method, on the other hand, is more often applied to the problem of solving conservation-type partial differential equations for various fluid flows, because of its advantages in dealing with irregular geometries and complex boundary conditions.

Ansys 2022R1 was used in this paper, from which the Flunet 2022R1 package has been widely recognized and used in the field of fluid computation. In this paper, a structured grid combined with the finite volume method was used to discretize the computational region, by integrating and linearizing the differential equations in each control volume to obtain a set of algebraic equations for the unknown variables, such as velocity, pressure, and turbulence energy, and then solving the system of equations. The system of equations of motion for each fluid can be written in the following generalized form:

$$\frac{\partial \phi}{\partial t} + \nabla \cdot (u_i \phi) = \nabla \cdot (\Gamma_\phi \nabla \phi) + S_\phi \tag{8}$$

where ϕ is a generic variable that can be used to represent variables such as velocity, turbulent kinetic energy, etc., Γ_ϕ is the diffusion coefficient of ϕ, and S_ϕ is the source term of the equation.

In this paper, the pressure–velocity coupling algorithm, which is commonly used to solve incompressible fluid dynamics problems, was used. Convergence can be achieved with fewer iterations than with separation algorithms such as SIMPLE (semi-implicit method for pressure-linked equations) in steady-state calculations. In the spatial discretization method, the least-squares cell-based gradient method was used. The PRESTO! (pressure-staggering option) scheme was chosen for pressure interpolation and the modified HRIC (high-resolution interface-capturing) scheme was used for volume fraction interpolation. The QUICK (quadratic upstream interpolation for convective kinetics) scheme, which is more accurate in quadrilateral grid solving, was chosen for the interpolation of momentum, turbulent kinetic energy, and dissipation rate.

In this paper, the conservation of water flux in the monitoring results was used to determine whether the calculations converged or not, which were considered to be converged when the flux error was below 0.1%.

3. Flood Intrusion in Underground Spaces and Staircases Model

3.1. Computational Meshing

According to China's Subway Design Code [55], a 26°34′ inclination angle is appropriate for staircases in subway stations, each staircase flight should not exceed 18 steps, and the length of the rest platform should be not less than 1.2 m. In this paper, the common occurrence of 14 steps for each staircase flight was used, each step was 0.3 m long and 0.15 m high, and the rest platform length was set to 1.2 m; considering the limit conditions and common situations, the model was established in 1:1 scale (Figure 3).

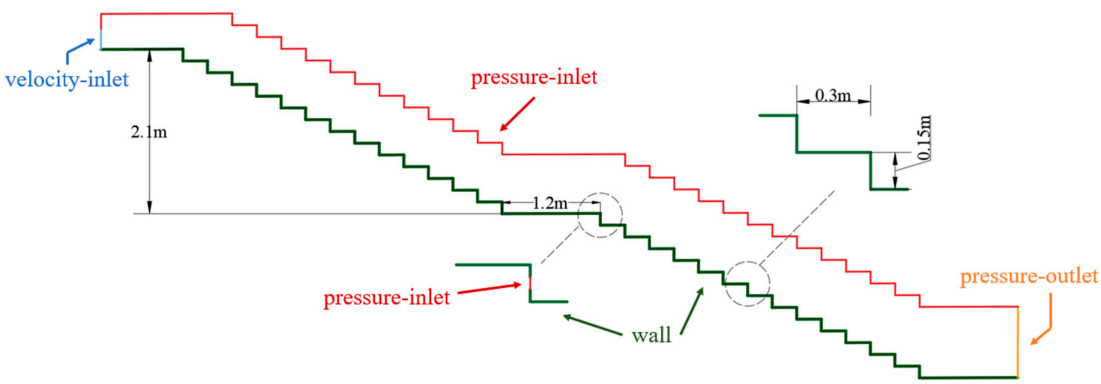

Figure 3. Schematic of staircase model construction and boundary condition setting.

In order to make the pressure in the upper part of the model always the same as the atmospheric pressure, the boundary condition of the upper part of the model was set as a gas-phase pressure-inlet, the boundary condition of the water inlet at the lower part of the entrance was set as a liquid-phase velocity-inlet, and the boundary condition of the exit of the staircase was set as a pressure-outlet. In order to simulate the water flow through the rest platform and the jet phenomenon generated downstream of the platform, the cavity in the lower part of the jet needed to be simulated by means of air replenishment [28], so the ventilation for the gas-phase pressure-inlet boundary condition was set in the middle of the first step riser under the platform (Figure 3). The volume fraction α = 0 was initially set in the computational domain, i.e., the initial domain was filled with air.

Considering that the entrance and exit platforms of subway stations are elevated above ground level, Jiang [28] derived the relationship between the flood height h_0 and the unit width flow q, based on the measurement results of the flow rate in indoor experiments of flooded staircases at different heights (Equation (9)), as follows:

$$q = 1.417{h_0}^{1.5} \tag{9}$$

In this paper, according to the relationship between unit width flow and inlet velocity, the relationship between inlet velocity v_0 and flood height h_0 (Equation (10)) was obtained with reference to Equation (9), and the liquid-phase inlet velocity v_0 boundary condition of the model was set accordingly, as follows:

$$v_0 = 1.417{h_0}^{0.5} \tag{10}$$

Jiang [28] and Hou, Chen [30] conducted a grid independence verification for the calculation of the staircase water flow model and analyzed the effect of grid size on the accuracy of simulation results, finding that setting the maximum grid size to 10 mm can best satisfy the computational accuracy and computational cost. In this paper, the computational domain was meshed using a quadrilateral structured grid, and the maximum grid size was set to 10 mm (Figure 4).

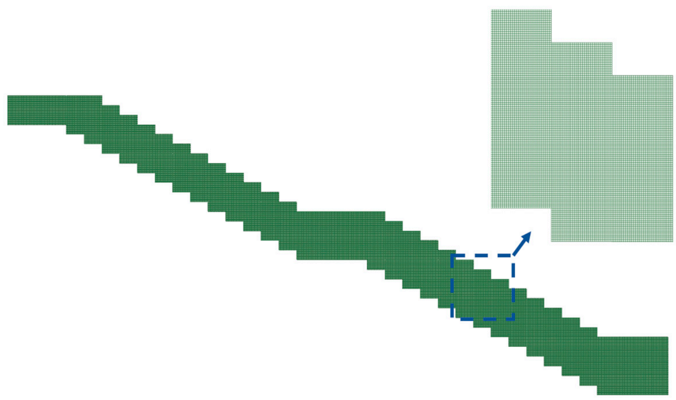

Figure 4. Meshing of the staircase model.

3.2. Definition of Flood Flow Velocity and Flood Height on the Staircase

As the flood flow velocity at the water–air interface is faster, the flow velocity at the water–air interface is often used as the calculation parameter when analyzing the risks of water flow on people escaping via the staircases. Therefore, the flow velocity of the subsequent analysis in this paper was taken as the flow velocity on the water–air interface, and the height of the water flow was taken as the height difference from the step boundary to the water–air interface. In addition, when the jet occurred downstream of the rest platform and the cavity appeared underneath it, the flow velocity was taken as the flow velocity at the upper water–air interface, and the height of the flow was taken as the height difference between the upper and lower water–air interfaces (Figure 5).

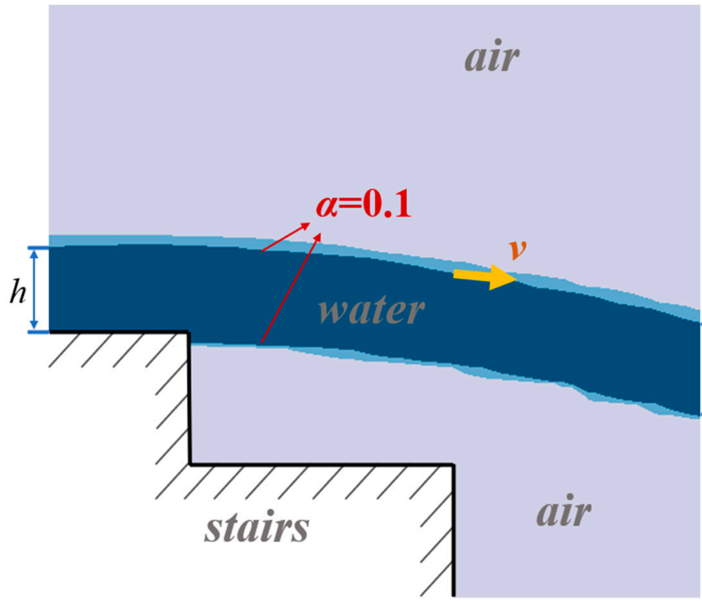

Figure 5. Illustration of flood flow velocity and flood height definition on staircase.

3.3. Model Validation

Water flow velocity not only directly affects the flow pattern of water, but also is the most important factor that prevents people from escaping using the staircase, which is often used as the focus in the staircase flooding analyses; therefore, the model validation and subsequent analysis of the calculation results in this paper were carried out using the flow velocity index.

Ishigaki, Toda [24] obtained flow velocity measurements on the flood surface at several steps when flood heights of 0.2 m, 0.3 m, and 0.4 m flowed into a long straight-running staircase without rest platforms in an indoor experiment. In this paper, simulations were performed under the same working conditions, based on the modeling method introduced in the previous section, and simulation results similar to the indoor experiment data were obtained (Figure 6).

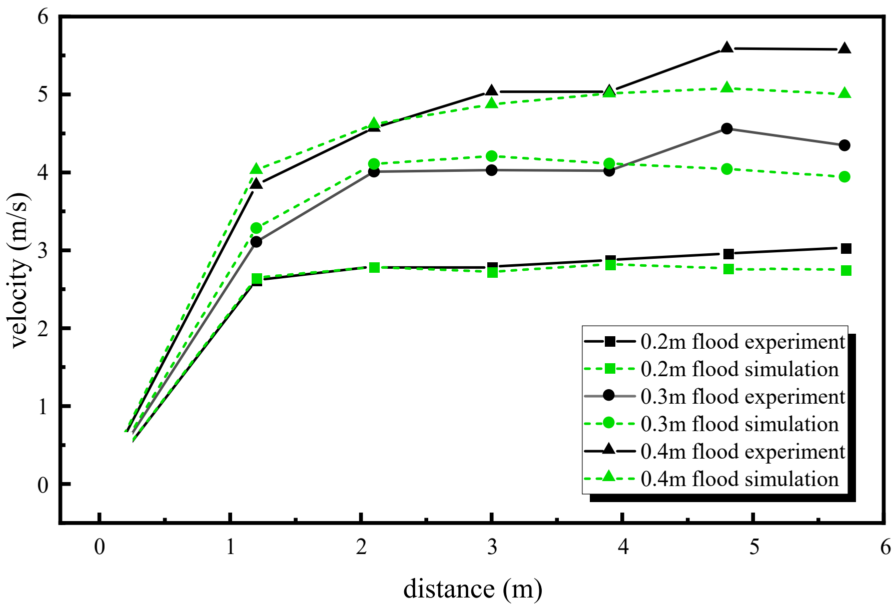

Figure 6. Simulated flow velocity results on staircase without rest platforms, compared to indoor experiment measurement data.

In this paper, the Nash–Sutcliffe efficiency coefficient (NSE), which is often used to validate hydrological model simulation results, was used to verify whether the simulated flow velocity results corresponded to the previous measurements (the closer the value was to one, the higher the confidence of the simulation results was). Compared to the results of Ishigaki, Toda, the NSE of the simulated flow velocity on the staircase at flood heights of 0.2 m, 0.3 m, and 0.4 m flood heights were 0.982, 0.966, and 0.972, respectively.

Jiang [28] simulated the flow characteristics on the edge surface of several steps when a 30cm high flood intruded onto a staircase with one rest platform at a scale of 1:2 and verified them by comparing with the results of an indoor experiment at the same scale. In this paper, based on the modeling method introduced in the previous section, the same 1:2 scale model was built and simulated under the same working conditions, similar simulation results were obtained (Figure 7). In comparison to Jiang's measurements, the simulation of water flow velocity on the staircase with a rest platform resulted in an NSE of 0.989. It can therefore be shown that the model construction calculation and mesh partitioning method, etc. used in this paper were valid.

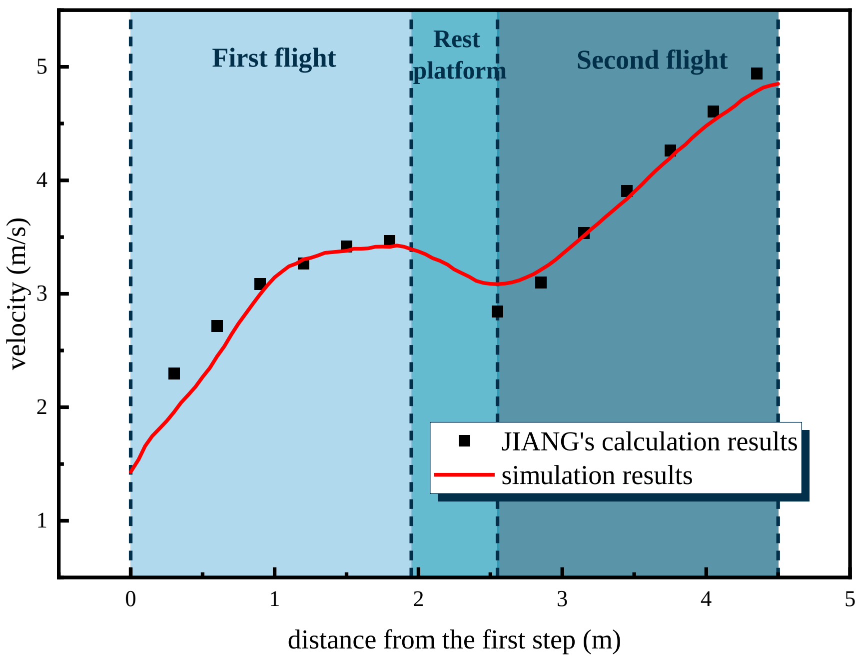

Figure 7. Simulation results of flow velocity on a staircase with one rest platform, compared to the results calculated by Jiang [28].

3.4. Case Settings

Considering the effects of different heights of the staircase, i.e., with different numbers of rest platforms, and different flood intrusion heights on the flow patterns and risks for people escaping on the staircase, six cases were set up in this paper, based on the number of rest platforms (number of stair flights minus one) and flood intrusion heights as variables. In addition, in order to simulate and calculate the influence of the rest platform on the flood flow pattern on the staircase and the flow characteristics of the flood water on the staircase, the model case, without a rest platform at the same total staircase height, was set. A total of seven cases are shown in Table 1 below.

Table 1. Simulated case settings.

No.	Number of Rest Platforms (pcs)	Total Height of Staircase (m)	Flood Intrusion Height (m)
1	2	5.85	0.3
2	3	7.8	0.3
3	4	9.75	0.3
4	4	9.75	0.25
5	4	9.75	0.2
6	4	9.75	0.15
7	0	9.75	0.3

4. Calculation of Results and Analysis

4.1. Effect of Rest Platform Setting on the Flow Pattern

In this paper, the effect of setting rest platforms on the flood flow velocity was analyzed by separately calculating the staircase model with four rest platforms (Case 3) and the continuous staircase model without rest platforms (Case 7) under the condition that the total height of the staircase is both 9.75 m, according to the Chinese Subway Design Code [55]. Taking the first step of the first flight as step number 1, the flow velocity variation curves on the edge of steps 1 to 70 were plotted (Figure 8a). It can be seen that, in the calculation results of the continuous staircase model without rest platforms, the flow velocity does not increase with the downward flow after reaching a certain velocity, due to the obstruction of the continuous step tread boundary (Figure 8c); this flow characteristic was also reflected in existing studies [24,28–30]. In the calculation of the staircase model with multiple rest platforms, although the rest platforms slowed down the water velocity in the area near the rest platform, the jet flow phenomenon caused by the rest platform (Figure 8b) substantially increased the flow velocity on the flights downstream of the platform, resulting in an overall increasing trend of the flow velocity on the staircase. A comparative analysis of the results shows that the calculated flow velocity on the downstream staircase after the 2nd flight was significantly higher than that of the continuous staircase model without rest platforms, which would have had a great effect on the analysis of the people escape hazard. Therefore, for the common case of subway station entrances and exits in underground flooding accidents, the continuous staircase model without rest platforms is suitable for simulating the water flow characteristics on staircases, but not for simulating the water flow characteristics on the downstream flights. Since the people escaping from the subway entrances and exits are more likely to escape using the staircase, it is necessary to analyze the model of a staircase with rest platforms.

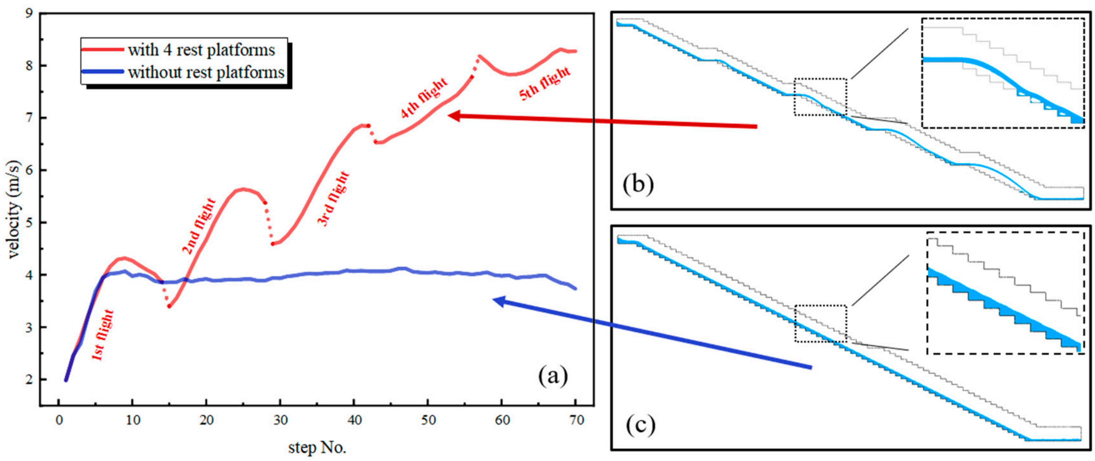

Figure 8. Effect of whether there are rest platforms: (**a**) velocity distribution, (**b**) water distribution with rest platforms, (**c**) water distribution without rest platforms.

4.2. Effect of the Number of Rest Platforms on the Flood Flow Pattern

In this paper, a 0.3 m flood height was simulated and calculated to intrude the staircase with two, three, and four rest platforms, respectively, the total staircase heights of which were 5.85 m, 7.8 m, and 9.75 m (Cases 1–3), and the variation in flood flow velocity on each location of the staircase, including the rest platform, was measured and plotted (Figure 9). It can be seen that, in the first four flights, the flow velocity of the three cases changed in a similar pattern: in each flight and rest platform range, the flow velocity first continued to increase and then continued to decrease, the flow velocity on the flights continued to increase to the middle or lower level of the flight, and then continued to decrease until the end of the rest platform; that is, the first step of the next flight. In addition, in terms of flow velocity values, the three cases were also very similar in the first four flights; the distribution settings of the staircase downstream did not affect the flow pattern on the staircase upstream, and the water intrusion simulation of the staircase with more rest platforms can characterize the flow pattern on the staircase with fewer rest platforms, so this paper follows with the higher staircase with four rest platforms as the object of simulation analysis.

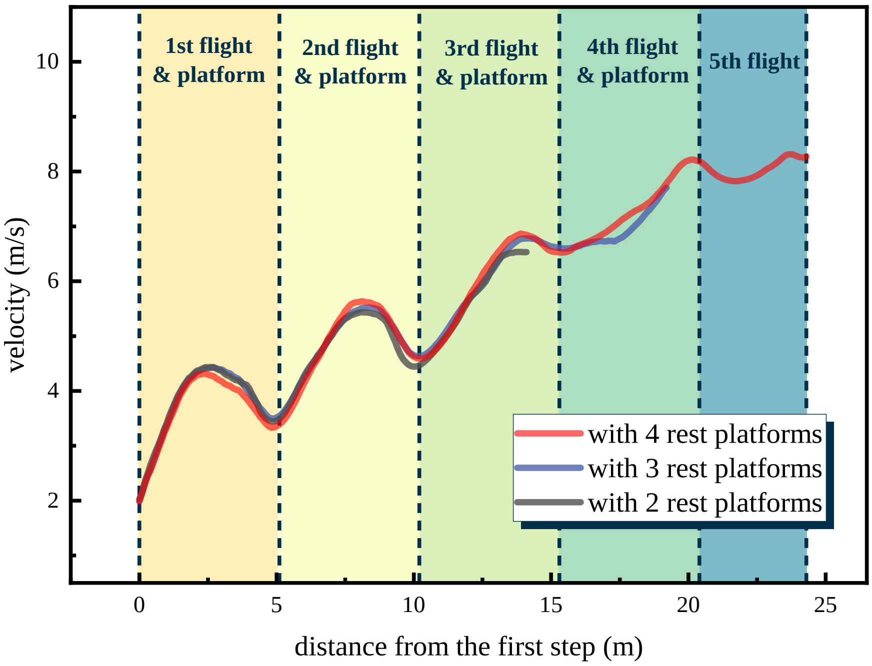

Figure 9. Variation in flow velocity on staircases with 2, 3 and 4 rest platforms.

4.3. Analysis of Flow Velocity Variation Patterns at Different Flood Heights

In this paper, the flow velocity variation results of 0.3, 0.25, 0.2, and 0.15 m high floods on the staircase with four rest platforms were simulated and calculated, respectively (Figure 10). It can be seen that, in all cases, the effect of the rest platforms on the flow velocity was consistent with the analysis in Section 4.1: it decreased first and then increased. Due to the acceleration by the platform jet and the deceleration by the step tread, the peak flow velocity of each step of each case basically appeared in the middle of the flight, where the two effects were balanced. Among them, the flow velocity variation for the 0.3 m and 0.25 m high floods was similar, as the overall flow velocity was fluctuating and increasing; while the flow velocity variation of 0.2 m and 0.15 m high floods was similar, the overall flow velocity fluctuated in a certain range and even had a tendency to decrease. The phenomenon was due to the higher flood, which had a faster initial flow velocity and a higher flow rate past the first step, which resulted in a longer distance of the jet [56]. Compared to the lower velocity flood flows, the faster flood flows were less impeded by the step boundary because of the longer jet distance, so the overall trend of flow velocity change was more dominated by the acceleration generated by the jet. This phenomenon was more evident after the flood passed through the second rest platform: the flood flow velocity was faster with a higher flood height, and the jet distance after the flood passed through the rest platform was longer (Figure 10a–c); with a lower flood height, the flood flow was slower, and the jet distance after the flood passed through the resting platform was shorter (Figure 10d–f).

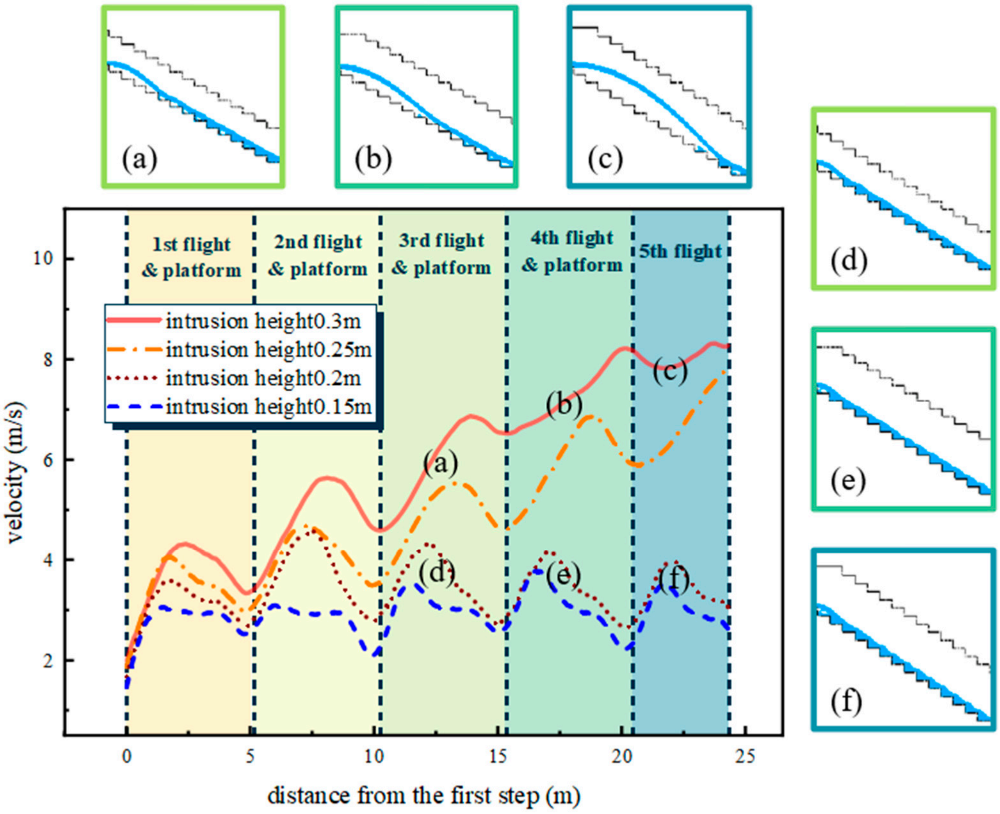

Figure 10. Variation in flow velocity on the staircase for different intrusion flood heights. (**a**–**c**) Jets on the 3rd to 5th flights at higher flood height, (**d**–**f**) Jets on the 3rd to 5th flights at lower flood height.

For each flight of staircases, a higher inlet velocity will result in a higher peak velocity v_{m} and a lower peak velocity point. A position factor δ was assumed to characterize the relative position of the peak velocity point on each flight, as follows:

$$\delta = \frac{l - \mathrm{L}}{\mathrm{L}} \tag{11}$$

where l is the horizontal distance between the peak velocity point and the edge of the first step of the flight and L is the sum of the horizontal length of the flight and the rest platform, which is 5.1 m in the model of this paper. Analyzing the relationship between the peak velocity v_{m} and the peak velocity point location coefficient δ for each case, it was found that the two were approximately linear (Figure 11). A linear fit curve of the two was derived (Equation (12)), and the resulting goodness of fit R^2 was 0.937, as follows:

$$v_{\mathrm{m}} = 6.64\delta + 1.7448 \tag{12}$$

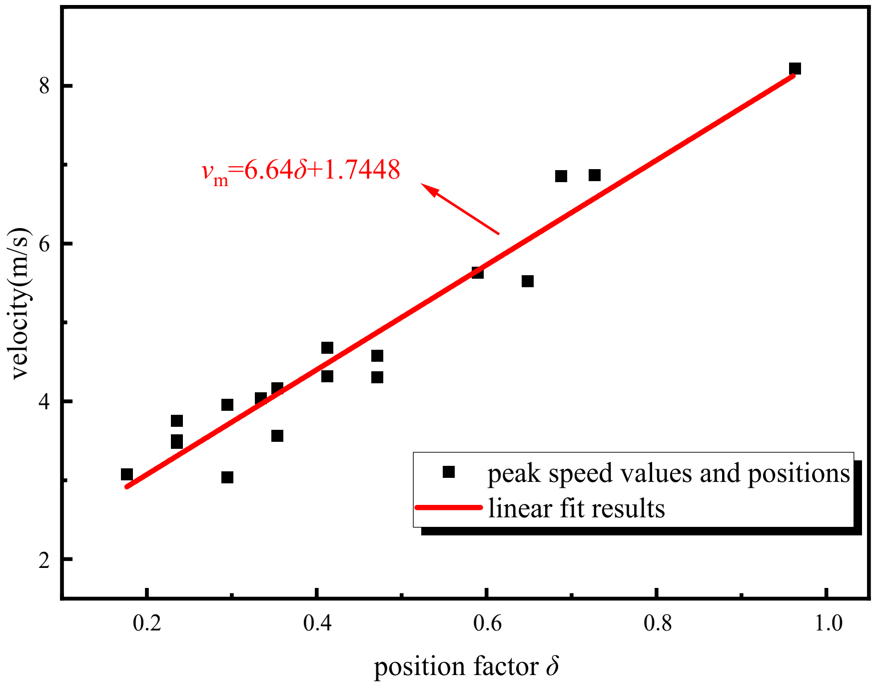

Figure 11. Fitting of peak velocity v_m versus position factor δ.

4.4. Hazards of Escaping for People in Flood Intrusion Staircase Accidents

When the ground material is consistent, the height and velocity of the flood water is the most important influence on the stability of people walking in the flood [57]. Ishigaki, Ozaki [58] set up escape tests for a variety of people in floods based on these two indicators and derived the escape judgment function (see Equation (2), given again below) and the critical escape conditions for each type of person, which are summarized, in this paper, for each type of person alone (Table 2).

Table 2. The conditions needed for each type of person to escape alone.

People Type	Escape Function $F(v,h)$
stronger people	$\leq$0.25
general people	$\leq$0.2
thinner people	$\leq$0.16

Since it is more difficult for people to escape up the steps during a flood than to the rest platform, and the flood flow velocity on the rest platform is lower, this paper calculated and plotted the change in escape function $F(v,h)$ on the edge surface of each step of a staircase with four rest platforms during 0.3, 0.25, 0.2, and 0.15 m high floods (Figure 12), and the curve between the two break points in the figure represents a flight. It can be seen that the change trend of escape function $F(v,h)$ for each case was similar to the change trend of flow velocity, which was due to the small change in flood height, and the increase in escape function $F(v,h)$ for the flood heights of 0.3 and 0.25 m was more obvious after the 3rd flight. For the flood height of 0.3 m, it was difficult for the thinner people to escape alone on the second half of the first flight, and the escape function $F(v,h)$ increased rapidly after the first rest platform, which seriously hindered the escape of all types of people; for the flood height of 0.25 m, all types of people could escape alone in the first flight but only the stronger people could escape alone on the second flight. After the 3rd flight, it was difficult for all kinds of people to escape alone; for the flood height of 0.2 m, only the thinner people in the 2nd and 3rd flights could hardly escape alone, while the rest of the people could escape; for the flood height of 0.15 m, all types of people could escape alone on each flight. Unlike for the flood height above 0.25 m, when the flood height was below

0.2 m, the escape function $F(v,h)$ did not increase significantly with the falling flow, but decreased and stabilized within the critical condition that each type of person could escape alone.

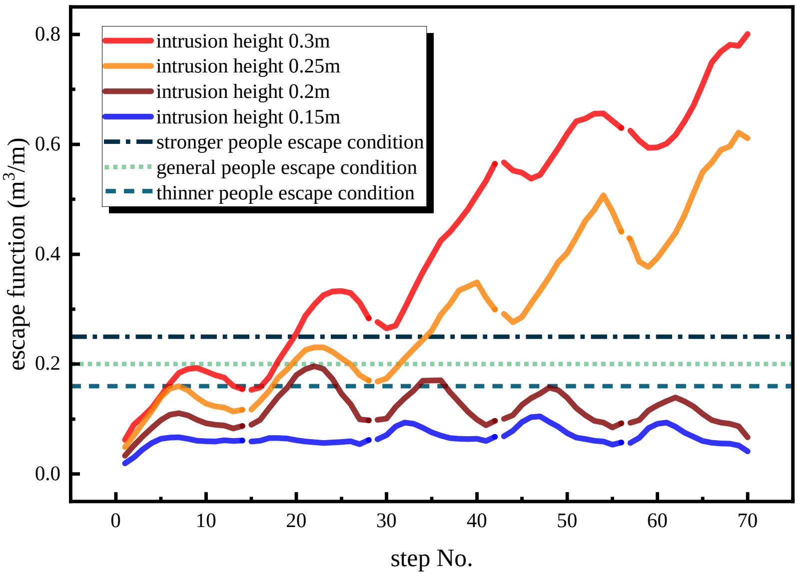

Figure 12. Variation in escape function $F(v,h)$ on each step for different flood height cases.

This shows that, in an underground flooding accident, when people escape on the common staircases with multiple rest platforms, it would seriously affect the escape of people in the downstream sections of the staircase if the height of the flood water, that is, the height of the ground flood, exceeds the height of the entrance and exit ground platforms by 0.2 m, and that the evacuation of people should be carried out before the height of the intrusion flood reaches 0.2 m. On the other hand, for cases where the height of the flood is higher than 0.2 m, people should evacuate to the first rest platform of the staircase as soon as possible; otherwise, people should look for temporary refuges or wait for rescue in places at a higher ground level within the underground structure, in order to avoid more serious damage from falling down the staircase.

5. Discussion of Results

In this paper, the RANS method was used to solve the turbulence model, and the VOF model was used to trace the free surface at the junction of flood water and air, i.e., the free water surface of the flood water on the staircase. This method is faster and less expensive than the direct turbulence modeling method, and it is able to calculate and analyze the flow distribution pattern of the flood water on the staircase at the same time. The calculated results are similar to the flow rate measurements of Ishigaki, Toda [24] and Jiang [28].

In contrast to the existing research papers, this paper focused on the effect of rest platform settings on the flow regime of floodwater over staircases. The staircases with multiple rest platforms discussed in this paper are more commonly found at the entrances and exits of existing underground facilities, and the proposed escape recommendations can be more widely generalized.

6. Conclusions

(1) Settings of rest platforms will cause the flow velocity in front of the platforms to decrease, but after the rest platforms, a jet flow will be generated, causing the water flow velocity to increase. For higher flood heights, the overall flow velocity showed a significant upward trend, which was different from the simulation results of the staircase model without rest platforms.

(2) By simulating the flooding of staircase models with two, three, and four rest platforms at the flood height of 0.3 m, it was concluded that the flow velocities and the changes on the first four flights were similar for the three cases; therefore, the staircase model with more rest platforms can be used to represent the staircase model with fewer rest platforms.
(3) The flow velocity variation results for 0.3, 0.25, 0.2, and 0.15 m high floods on staircases with four rest platforms were calculated and analyzed, respectively; it is found that the peak velocity v_m and the peak velocity point location coefficient δ of the flood on the staircases in each case were approximately linear, and the linear relationship equation between them was derived.
(4) Based on the escape function, the critical escape conditions for various types of people under different cases were calculated and analyzed. It was concluded that when the height of the flood, i.e., the height of the ground flood water, exceeded 0.2 m above the height of the ground platform at the entrance and exit, the escape of people on the downstream sections of the staircase will be seriously affected; the evacuation of people should be carried out before the height of the flood reaches 0.2 m, as far as possible.

Author Contributions: Methodology, Z.L., S.H. and H.L.; Software, S.H.; Validation, Z.L. and H.L.; Formal analysis, Z.L. and H.L.; Writing—original draft, Z.L., S.H. and H.L.; Writing—review & editing, Z.L., S.H. and H.L. All authors have read and agreed to the published version of the manuscript.

Funding: This paper obtained funding from the Postgraduate Innovative Project (2021) of Study on Flood Disaster Prevention Model of Nanning Rail Transit. The authors wish to acknowledge this support.

Data Availability Statement: Some or all data, models, or code that support the findings of this study are available from the corresponding author upon reasonable request.

Conflicts of Interest: Author Shengbin Hu was employed by the company Nanning Rail Transit Co., Ltd. The remaining authors declare that the research was conducted in the absence of any commercial or financial relationships that could be construed as a potential conflict of interest.

References

1. UN Office for Disaster Risk Reduction. *The Human Cost of Disasters: An Overview of the Last 20 Years (2000–2019)*; UNDRR: Geneva, Switzerland, 2020.
2. Li, G.; He, X.; Li, M.; Wang, Z.; Wu, S.; Jiang, Y.; Wu, J.; Chen, W. Experimental study on treatment of disintegrating rock under expansive soil slope at Yangtze-to-Huaihe water diversion project. *Zhongnan Daxue Xuebao (Ziran Kexue Ban)/J. Cent. South Univ. (Sci. Technol.)* **2022**, *53*, 51–74. [CrossRef]
3. Custer, R.; Nishijima, K. Probabilistic disaggregation of a spatial portfolio of exposure for natural hazard risk assessment. *Georisk-Assess. Manag. Risk Eng. Syst. Geohazards* **2018**, *12*, 1–13. [CrossRef]
4. Liu, W.; Feng, Q.; Engel, B.A.; Yu, T.; Zhang, X.; Qian, Y. A probabilistic assessment of urban flood risk and impacts of future climate change. *J. Hydrol.* **2023**, *618*, 129267. [CrossRef]
5. Luo, K.S.; Zhang, X.J. Increasing urban flood risk in China over recent 40 years induced by LUCC. *Landsc. Urban Plan.* **2022**, *219*, 104317. [CrossRef]
6. Miller, J.D.; Hutchins, M. The impacts of urbanisation and climate change on urban flooding and urban water quality: A review of the evidence concerning the United Kingdom. *J. Hydrol. -Reg. Stud.* **2017**, *12*, 345–362. [CrossRef]
7. Han, J.; Wang, C.; Deng, S.; Lichtfouse, E. China's sponge cities alleviate urban flooding and water shortage: A review. *Environ. Chem. Lett.* **2023**, *21*, 1297–1314. [CrossRef]
8. Huong, H.T.L.; Pathirana, A. Urbanization and climate change impacts on future urban flooding in Can Tho city, Vietnam. *Hydrol. Earth Syst. Sci.* **2013**, *17*, 379–394. [CrossRef]
9. Pallathadka, A.; Sauer, J.; Chang, H.E.J.; Grimm, N.B. Urban flood risk and green infrastructure: Who is exposed to risk and who benefits from investment? A case study of three US Cities. *Landsc. Urban Plan.* **2022**, *223*, 104417. [CrossRef]
10. Wang, Y.; Chen, S.; Ouyang, J.; Li, J.; Zhao, Y.; Lin, H.; Guo, P. Predicting ground surface settlements induced by deep excavation under embankment surcharge load in flood detention zone. *Water* **2022**, *14*, 3868. [CrossRef]
11. China Association of Metros. *Urban Rail Transit 2021 Annual Statistics and Analysis Report*; China Association of Metros: Beijing, China, 2022.

12. Shin, E.; Kim, H.-J.; Rhee, D.S.; Eom, T.; Song, C.G. Spatiotemporal flood risk assessment of underground space considering flood intensity and escape route. *Nat. Hazards* **2021**, *109*, 1539–1555. [CrossRef]
13. Han, Y.S.; Shin, E.T.; Eum, T.S.; Song, C.G. Inundation Risk Assessment of Underground Space Using Consequence-Probability Matrix. *Appl. Sci.* **2019**, *9*, 1196. [CrossRef]
14. Shao, W.-Y. Critical rainfall intensity for safe evacuation from underground spaces with flood prevention measures. *J. Zhejiang Univ. -Sci. A* **2010**, *11*, 668–676. [CrossRef]
15. Wang, D.; Ye, S.; Zhang, J. Risk Reduction Measures and Monitoring Analysis of Deep Foundation Pit with Water in a Metro Station in Hefei. *Water* **2023**, *15*, 3007. [CrossRef]
16. Gonzva, M.; Barroca, B.; Gautier, P.-É.; Diab, Y. Modeling disruptions causing domino effects in urban guided transport systems faced by flood hazards. *Nat. Hazards* **2017**, *86*, 183–201. [CrossRef]
17. Robert, B.; De Calan, R.; Morabito, L. Modelling interdependencies among critical infrastructures. *Int. J. Crit. Infrastruct.* **2008**, *4*, 392–408. [CrossRef]
18. Yu, Z.; Zhu, X.; Liu, X. Characterizing metro stations via urban function: Thematic evidence from transit-oriented development (TOD) in Hong Kong. *J. Transp. Geogr.* **2022**, *99*, 103299. [CrossRef]
19. Su, S.L.; Zhao, C.; Zhou, H.; Li, B.Z.; Kang, M.J. Unraveling the relative contribution of TOD structural factors to metro ridership: A novel localized modeling approach with implications on spatial planning. *J. Transp. Geogr.* **2022**, *100*, 103308. [CrossRef]
20. Takahashi, T.; Nakagawa, I.; Nomura, D. Simulation method on inundation in an underground space due to intrusion of overland flood flows. *Annu. Disaster Prev. Res. Inst. Kyoto Univ.* **1990**, *33*, 427–442.
21. Tang, Y.; Zhou, T.; Zhong, Y.; Hu, S.; Lin, J.; Lin, Z.; Liu, H.; Liu, B.; Zhao, Y.; Wang, Y.; et al. Risk assessment for critical flood height of pedestrian escape in subway station. *Water* **2022**, *14*, 3409. [CrossRef]
22. Lin, Z.; Hu, S.; Zhou, T.; Zhong, Y.; Zhu, Y.; Shi, L.; Lin, H. Numerical simulation of flood intrusion process under malfunction of flood retaining facilities in complex subway stations. *Buildings* **2022**, *12*, 853. [CrossRef]
23. Inoue, K.; Toda, K.; Nakai, T. Simulation on the Inundation Process in the Underground Space. *Annu. Rep. Disaster Prev. Res. Inst. Kyoto Univ.* **2003**, *46*, 263–273.
24. Ishigaki, T.; Toda, K.; Baba, Y.; Inoue, K.; Nakagawa, H. Experimental study on evacuation from underground space by using real size models. *Proc. Hydraul. Eng.* **2006**, *50*, 583–588. [CrossRef]
25. Ishigaki, T.; Asai, Y.; Nakahata, Y.; Shimada, H.; Baba, Y.; Toda, K. Evacuation of aged persons from inundated underground space. *Water Sci. Technol.* **2010**, *62*, 1807–1812. [CrossRef] [PubMed]
26. Wu, J.; Bao, K.; Zhang, H.; Yang, R. Numerical model of staircase flow based on the SPH method. *J. Tsinghua Univ. Sci. Technol.* **2011**, *51*, 7.
27. Shao, W.; Jiang, L.; Zhang, Y.; Zhu, D.Z.; Sun, Z.-L. Hydraulic features of air-water mixture flow on a staircase with rest platforms. *J. Hydraul. Eng.* **2014**, *140*, 04014016. [CrossRef]
28. Jiang, L. Features of Hydraulics and Flow Past Cvlinder(s) on Staircase. Ph.D. Thesis, Zhejiang University, Hangzhou, China, 2014.
29. Kim, M.; Lee, D.H.; Kim, J.-S.; Eom, J.H. A Study on Evacuation Safety at Inundated Stairs by using Real-scale Hydraulic Model Experiment. *E3S Web Conf.* **2018**, *40*, 06016. [CrossRef]
30. Hou, J.; Chen, G.; Zhang, Y.; Li, B.; Yang, S.; Tong, Y.; Zhang, D.; Fu, D. A simulation study on risks of pedestrian evacuation from flooded staircases of different slopes in the underground space. *Nat. Hazards* **2022**, *110*, 519–543. [CrossRef]
31. Li, Q.; Xia, J.; Xie, Z.; Zhou, M.; Deng, S. Hazard and vulnerability in urban inundated underground space: Hydrodynamic analysis of human instability for stairway evacuation. *Int. J. Disaster Risk Reduct.* **2022**, *70*, 102754. [CrossRef]
32. Gao, R.G.; Wang, W.J.; Zhou, K.P.; Zhao, Y.L.; Yang, C.; Ren, Q.F. Optimization of a Multiphase Mixed Flow Field in Backfill Slurry Preparation Based on Multiphase Flow Interaction. *Acs Omega* **2023**, *8*, 34698–34709. [CrossRef] [PubMed]
33. Farhana, K.; Mahamude, A.S.F.; Kadirgama, K. Numerical study of solar tray with noble Mxene nanofluids. *J. Cent. South Univ.* **2023**, *30*, 3656–3669. [CrossRef]
34. Aslam, M.N.; Riaz, A.; Shaukat, N.; Ali, S.; Akram, S.; Bhatti, M.M. Analysis of incompressible viscous fluid flow in convergent and divergent channels with a hybrid meta-heuristic optimization techniques in ANN: An intelligent approach. *J. Cent. South Univ.* **2023**, *30*, 4149–4167. [CrossRef]
35. Rodi, W. Turbulence Modeling and Simulation in Hydraulics: A Historical Review. *J. Hydraul. Eng.* **2017**, *143*, 03117001. [CrossRef]
36. Qian, Z.D.; Hu, X.Q.; Huai, W.X.; Amador, A. Numerical simulation and analysis of water flow over stepped spillways. *Sci. China Ser. E-Technol. Sci.* **2009**, *52*, 1958–1965. [CrossRef]
37. Kositgittiwong, D.; Chinnarasri, C.; Julien, P.Y. Numerical simulation of flow velocity profiles along a stepped spillway. *Proc. Inst. Mech. Eng. Part E J. Process Mech. Eng.* **2013**, *227*, 327–335. [CrossRef]
38. Biscarini, C.; Di Francesco, S.; Manciola, P. CFD modelling approach for dam break flow studies. *Hydrol. Earth Syst. Sci.* **2010**, *14*, 705–718. [CrossRef]
39. Guo, X.-Y.; Jiang, B.-C.; Chen, J.-H.; Wang, Q.-M. Effect of oxygen lance seat arrangement on flow characteristics of large-scale copper smelting bottom-blown furnace. *J. Cent. South Univ.* **2023**, *30*, 2542–2555. [CrossRef]
40. Du, J.; Liang, X.-F.; Li, G.-B.; Tian, H.-L.; Yang, M.-Z. Numerical simulatim of rainwater accumulation and flow characteristics over windshield of high-speed trains. *J. Cent. South Univ.* **2020**, *27*, 198–209. [CrossRef]
41. Choi, J.; Yoon, S.B. Numerical simulations using momentum source wave-maker applied to RANS equation model. *Coast. Eng.* **2009**, *56*, 1043–1060. [CrossRef]

42. Zhao, Q.; Armfield, S.; Tanimoto, K. Numerical simulation of breaking waves by a multi-scale turbulence model. *Coast. Eng.* **2004**, *51*, 53–80. [CrossRef]
43. Nezhadian, D.M.A.; Hamidifar, H. Effects of Floating Debris on Flow Characteristics around Slotted Bridge Piers: A Numerical Simulation. *Water* **2024**, *16*, 90. [CrossRef]
44. Chala, D.C.; Quinones-Bolanos, E.; Mehrvar, M. Land Subsidence Due to Groundwater Exploitation in Unconfined Aquifers: Experimental and Numerical Assessment with Computational Fluid Dynamics. *Water* **2024**, *16*, 467. [CrossRef]
45. Cheng, Y.; Yang, M.; Xie, S.; Liu, J.; Zheng, S. Research on the Impact of Air Temperature and Wind Speed on Ventilation in University Dormitories under Different Wind Directions (Northeast China). *Buildings* **2024**, *14*, 361. [CrossRef]
46. Marsooli, R.; Wu, W.M. 3-D finite-volume model of dam-break flow over uneven beds based on VOF method. *Adv. Water Resour.* **2014**, *70*, 104–117. [CrossRef]
47. Tongkratoke, A.; Chinnarasri, C.; Pornprommin, A.; Dechaumphai, P.; Juntasaro, V. Non-linear turbulence models for multiphase recirculating free-surface flow over stepped spillways. *Int. J. Comput. Fluid Dyn.* **2009**, *23*, 401–409. [CrossRef]
48. Chen, Q.; Dai, G.Q.; Liu, H.W. Volume of fluid model for turbulence numerical simulation of stepped spillway overflow. *J. Hydraul. Eng.* **2002**, *128*, 683–688. [CrossRef]
49. Yoneyama, N.; Toda, K.; Aihata, S.; Yamamoto, D. Numerical Analysis for Evacuation Possibility From Small Underground Space in Urban Flood. In *Advances in Water Resources and Hydraulic Engineering*; Zhang, C., Tang, H., Eds.; Springer: Berlin/Heidelberg, Germany, 2009; pp. 107–112.
50. Jiang, L.; Shao, W.; Zhu, D.Z.; Sun, Z. Forces on surface-piercing vertical circular cylinder groups on flooding staircase. *J. Fluids Struct.* **2014**, *46*, 17–28. [CrossRef]
51. Youngs, D. Time-Dependent Multi-material Flow with Large Fluid Distortion. *Numer. Methods Fluid Dyn.* **1982**, *24*, 273–285.
52. Wang, Y.; Gu, Y.; Liu, J. A domain-decomposition generalized finite difference method for stress analysis in three-dimensional composite materials. *Appl. Math. Lett.* **2020**, *104*, 106226. [CrossRef]
53. Kabir, H.; Aghdam, M.M. A generalized 2D Bézier-based solution for stress analysis of notched epoxy resin plates reinforced with graphene nanoplatelets. *Thin-Walled Struct.* **2021**, *169*, 108484. [CrossRef]
54. Bert, C.W.; Malik, M. Differential quadrature: A powerful new technique for analysis of composite structures. *Compos. Struct.* **1997**, *39*, 179–189. [CrossRef]
55. *GB 50157-2013*; Cord for Design of Metro. Beijing Urban Engineering Design & Research Institute Co. L.: Beijing, China, 2014.
56. Toombes, L.; Wagner, C.; Chanson, H. Flow patterns in nappe flow regime down low gradient stepped chutes. *J. Hydraul. Res.* **2008**, *46*, 4–14. [CrossRef]
57. Cao, L.; Zhong, G.; Lyu, S.; Wu, X. Analysis of Human Instability in Flood Flow. *J. Tongji Univ. (Nat. Sci.)* **2013**, *41*, 1675–1681.
58. Ishigaki, T.; Ozaki, T.; Inoue, T.; Shimada, H.; Toda, K. Drainage System, Rainwater Flooding and Underground Inundation in Urban Area. In Proceedings of the 12th International Conference on Urban Drainage, Porto Alegre, Brazil, 11–16 September 2011.